APPLYING DYNAMIC PROCEDURE FOR THE ENERGY PRODUCTION IN ONE-EQUATION SUBGRID SCALE MODEL OF LES

Takeo Kajishima, Takayuki Nomachi
Department of Mechanical Engineering,
Osaka University
Yamadaoka, Suita, Osaka 565-0871, Japan
kajisima@mech.eng.osaka-u.ac.jp

ABSTRACT

In order to develop a universal subgrid scale model for large-eddy simulation (LES), we take note of one-equation model for subgrid scale (SGS) kinetic energy, K_{SGS}. A dynamic procedure is used to the production term in the transport equation of SGS kinetic energy, while the eddy viscosity in the filtered equation of motion is determined indirectly through K_{SGS}. The statistically derived model for K_{SGS} equation is adopted for the basis of our improvement. First, our model was applied to a fully developed turbulent flow in a plane channel and agreement with DNS database was satisfactory. In addition, the influence of solid body rotation on a channel flow was compared. Our model, resolving a defect of conventional eddy viscosity models, reasonably reproduced the decay of SGS turbulence in the vicinity of the suction side.

INTRODUCTION

Smagorinsky model (1963) is still most popular SGS model in LES and has been used for wide variety of turbulent flows. It needs modifications in the non-turbulent region and in the vicinity of solid wall. This makes a barrier to universal utility. The dynamic Smagorinsky model proposed by Germano, et al. (1991) and modified by Lilly (1992), may overcome this problem by automatically adjusting the model parameter with the aid of resolved turbulence. The negative value of SGS eddy viscosity sometimes appears in the dynamic Smagorinsky model and it could be related to the energy backscatter from SGS to GS portion. It however should be removed in some way since it causes numerical instability. As a result, the aspect of the dynamic model is diminished in an actual application.

The authors proposed the utilization of the dynamic procedure in one-equation model of SGS kinetic energy (Kajishima and Nomachi, 2003). It is motivated through the reconsideration about what can be evaluated dynamically. In our method, the production of K_{SGS}, corresponding to the energy transfer from GS to SGS portion of turbulence kinetic energy, is determined through dynamic procedure. On the other hand, SGS stress in the filtered equation of motion is approximated by the eddy viscosity model and it is given indirectly by K_{SGS}. We used the theoretically derived one-equation SGS model by Yoshizawa and Horiuti (1985), Horiuti (1985) and then improved by Okamoto and Shima (1999) as a basis. Thus any ad hoc modification for the length scales is excluded.

Generally, the one-equation model has many notable merits. Thus it has been attracted attention (Ghosal, et al., 1995; Davidson, 1997; Sohankar, 2000). The SGS eddy-viscosity, being proportional to $\sqrt{K_{SGS}}\Delta$, does not become negative anywhere. K_{SGS} disappears automatically in non-turbulent region and it becomes zero on the solid wall due to the boundary condition. Moreover, wide variety of factors, such as non-equilibrium properties and additional energy sources or sinks such as particles or bubbles can be included.

First in the present paper, we apply our one-equation SGS model to a fully developed flow in a plane channel as a standard example. Results by our model and the existing model are compared with DNS database (Moser, et al., 1999). Second, the realizability of effect of Coriolis force in the rotating channel is examined. Especially in the suction side of rotating channel, Smagorinsky model gives SGS turbulence due to the mean velocity gradient even if GS flow is almost re-laminarized. We will demonstrate this issue is solved by our method.

BASIC EQUATIONS

Basic Equations for LES and Dynamic Smagorinsky Model

The density and viscosity of flow are assumed to be constant. The filtering operation is represented as

$$\bar{f}(\boldsymbol{x}) = \int_{-\infty}^{\infty} G(\boldsymbol{y}) f(\boldsymbol{x}-\boldsymbol{y}) d\boldsymbol{y}\,, \tag{1}$$

where G is the 'grid filter' function having the representative length corresponding to the width of computational grid. Basic equations for LES is the filtered Navier-Stokes equation of motion

$$\frac{\partial \bar{u}_i}{\partial t} + \bar{u}_j \frac{\partial \bar{u}_i}{\partial x_j} = -\frac{\partial \bar{P}}{\partial x_i} + \frac{\partial}{\partial x_j}(-\tau_{ij} + 2\nu \bar{S}_{ij}) \tag{2}$$

and the filtered continuity equation

$$\frac{\partial \bar{u}_i}{\partial x_i} = 0\,, \tag{3}$$

where $\bar{u}$ denotes the GS component of velocity, $\bar{p}$ (in $\bar{P} = \bar{p}/\rho$) the GS component of pressure, ρ the fluid density, ν the kinematic viscosity of fluid.

$$\bar{S}_{ij} = \frac{1}{2}\left(\frac{\partial \bar{u}_i}{\partial x_j} + \frac{\partial \bar{u}_j}{\partial x_i}\right) \tag{4}$$

represents the deformation rate tensor of GS flow field and $\tau_{ij} = \overline{u_i u_j} - \bar{u}_i \bar{u}_j$ is the SGS stress.

The 'test filter'

$$\tilde{f}(\boldsymbol{x}) = \int_{-\infty}^{\infty} \tilde{G}(\boldsymbol{y}) f(\boldsymbol{x}-\boldsymbol{y}) d\boldsymbol{y} \tag{5}$$

which has wider length scale than that of grid filter is introduced in the dynamic model. Applying the test filter to Eqs.(2) and (3) results in

$$\frac{\partial \tilde{\bar{u}}_i}{\partial t} + \tilde{\bar{u}}_j \frac{\partial \tilde{\bar{u}}_i}{\partial x_j} = -\frac{\partial \tilde{\bar{P}}}{\partial x_i} + \frac{\partial}{\partial x_j}(-T_{ij} + 2\nu \tilde{\bar{S}}_{ij}), \quad (6)$$

$$\frac{\partial \tilde{\bar{u}}_i}{\partial x_i} = 0, \quad (7)$$

where $T_{ij} = \widetilde{\bar{u}_i \bar{u}_j} - \tilde{\bar{u}}_i \tilde{\bar{u}}_j$ is the sub-test scale stress. The dybamic Smagorinsky applies the same eddy-viscosity assumption for τ_{ij} and T_{ij} as follows (Gernamo, et al., 1991):

$$\tau^a_{ij} (= \tau_{ij} - \frac{1}{3}\delta_{ij}\tau_{kk}) = -2C_S \bar{\Delta}^2 |\bar{S}| \bar{S}_{ij}, \quad (8)$$

$$T^a_{ij} (= T_{ij} - \frac{1}{3}\delta_{ij}T_{kk}) = -2C_S \tilde{\bar{\Delta}}^2 |\tilde{\bar{S}}| \tilde{\bar{S}}_{ij}, \quad (9)$$

where the superscript ^{a} denotes an anisotropic part of the tensor, $|\bar{S}| (= \sqrt{2\bar{S}_{nm}\bar{S}_{nm}})$ the strength of the tensor $\bar{S}_{ij}$. $\bar{\Delta}$ is the characteristic length of the grid filter G and $\tilde{\Delta}$ is that of the test filter $\tilde{G}$. The ratio $\alpha = (\tilde{\Delta}/\bar{\Delta})$ is a parameter in the dynamic Smagorinsky model. C_S is usually determined according to the least square method (Lilly, 1992)

$$2C_S \bar{\Delta}^2 = -\frac{L_{ij} M_{ij}}{M_{kl} M_{kl}}, \quad (10)$$

to minimize the error for Germano identity $L_{ij} (= T_{ij} - \tilde{\tau}_{ij}) = \widetilde{\bar{u}_i \bar{u}_j} - \tilde{\bar{u}}_i \tilde{\bar{u}}_j$, where $M_{ij} = \alpha^2 |\tilde{\bar{S}}| \tilde{\bar{S}}_{ij} - \widetilde{|\bar{S}| \bar{S}_{ij}}$.

One-Equation Dynamic Model

Applying the eddy viscosity assumption to the filtered equation of motion (2) results in

$$\frac{\partial \bar{u}_i}{\partial t} + \bar{u}_j \frac{\partial \bar{u}_i}{\partial x_j} = -\frac{\partial}{\partial x_i}\left(\bar{P} + \frac{2}{3}K_{SGS}\right) + \frac{\partial}{\partial x_j}\left[2(\nu_S + \nu)\bar{S}_{ij}\right]. \quad (11)$$

The SGS eddy viscosity ν_S can be given as

$$\nu_S = C_\nu \Delta_\nu \sqrt{K_{SGS}} \quad (12)$$

by the dimensional analysis, where $K_{SGS} (= \tau_{ij}/2)$ is the SGS kinetic energy. Since $C_\nu (> 0)$ is constant, ν_S cannot have negative value. Thus the computation of Eq.(11) is expected to be numerically stable. K_{SGS} is obtained by solving the transport equation

$$\frac{\partial K_{SGS}}{\partial t} + \bar{u}_j \frac{\partial K_{SGS}}{\partial x_j} = -\tau^a_{ij}\bar{S}_{ij} - C_\varepsilon \frac{K^{3/2}_{SGS}}{\bar{\Delta}} - \varepsilon_w + \frac{\partial}{\partial x_j}\left[(C_d \Delta_\nu \sqrt{K_{SGS}} + \nu)\frac{\partial K_{SGS}}{\partial x_j}\right], \quad (13)$$

which has been theoretically derived (Yoshizawa and Horiuti, 1985; Horiuti, 1985; Okamoto and Shima, 1999).

We propose a one-equation dynamic model in which the dynamic procedure, Eqs.(8)-(10), is applied to τ^a_{ij} in the energy production term, the first term in RHS of Eq.(13). This realizes the concept that the dynamic procedure is suitable for the energy transfer between GS and SGS component. On the other hand, the eddy viscosity ν_S in the equation of motion (11) is given by Eq.(12). Thus ν_S is indirectly influenced by the interaction between GS and SGS component of turbulence.

The SGS eddy viscosity ν_S becomes automatically zero on the solid wall in accordance with the boundary condition $K_{SGS} = 0$ at the wall. However, additional modification is necessary to meet the correct asymptotic behavior to the wall. The proposal by Okamoto and Shima (1999) is adopted here. The characteristic length Δ_ν in Eq.(12) is given by

$$\Delta_\nu = \frac{\bar{\Delta}}{1 + C_k \bar{\Delta}^2 \bar{S}^2 / K_{SGS}}. \quad (14)$$

This is considered to be a Pade approximation, to avoid the negative value, of the 3rd-order anisotropic representation (Horiuti, 1990; Horiuti, 1993). As for the dissipation term, the length scale is not modified but the additional term

$$\varepsilon_w = 2\nu \frac{\partial \sqrt{K_{SGS}}}{\partial x_j} \frac{\partial \sqrt{K_{SGS}}}{\partial x_j} \quad (15)$$

is used. This has the same formulation used in the low Reynolds number version of $k-\varepsilon$ model (Jones and Launder, 1972).

Any smoothing or averaging is not applied for C_S in our method. Even if C_S became negative, the stability of computation was maintained in our experience. The artificial handling was only the clipping of negative K_{SGS} ($\max[0, K_{SGS}] \to K_{SGS}$). This manipulation was unlikely to affect the numerical result because the rate of appearance was less than a few percent in the vicinity of wall and absolute values of negative K_{SGS} were very small.

The width of the grid filter $\bar{\Delta}_i$ is assumed to be same as that of the computational grid Δ_i. The width of the test filter $\tilde{\Delta}_i$ is twice of Δ_i. Non-dimensional constants are as follows; $C_\nu = 0.05$, $C_\varepsilon = 0.835$, $C_d = 0.10$ and $C_k = 0.08$. C_ν, C_ε and C_d are same as recommended values for channel flow (Okamoto and Shima, 1999). C_k is close to the theoretically derived value (0.0784).

As shown above, our model does not use any parameters that is difficult to be specified for the complicated geometries, such as friction velocity on the wall or distance from the wall. Considering the numerical stability and universality in model, we believe this dynamic procedure is applicable for wide variety of turbulence flow field.

LES OF FLOW IN PLANE CHANNEL

A fully developed flow in a plane channel, maintained by the constant pressure gradient, is considered in this section.

Outline of computation

The x, y and z represent streamwise, wall-normal and spanwise directions, respectively. The computational domain is $L_x = 6.4\delta$, $L_y = 2\delta$ and $L_z = 3.2\delta$ in each direction where δ is the channel half width. The periodic boundary condition is assumed in the homogeneous (x and z) directions. The non-slip boundary condition is

Table 1: Number of grid points and resolution

Re_τ	-	$N_x \times N_y \times N_z$	Δx^+	Δz^+	Δy_c^+
395	Case1	$32 \times 65 \times 32$	79.0	39.5	23.8
	Case2	$48 \times 65 \times 48$	52.7	26.3	23.8
	Case3	$64 \times 65 \times 64$	39.5	19.8	23.8
590	Case4	$48 \times 65 \times 48$	78.7	39.3	35.5
	Case5	$64 \times 65 \times 64$	59.0	29.5	35.5
	Case6	$96 \times 97 \times 96$	39.2	19.7	23.7

applied at the solid wall. We use the staggered arrangement of variables, being suitable for the incompressible fluid flow. The spatial derivative is approximated by the central finite-difference method of the 4th order accuracy. The time-marching method is SMAC scheme, using the 2nd-order Adams-Bashforth method for the prediction step. To solve the Poisson equation of pressure, the FFT method is applied into the periodic directions and the LU decomposition method in the wall-normal direction.

The Reynolds numbers based on δ and the mean friction velocity at the wall u_τ are $Re_\tau(=\delta u_\tau/\nu)$ =395 and 590, which is corresponding to the DNS database (Moser, et al. 1999). To observe the influence of grid resolution, mainly 3 steps of computational size as shown in Table 1 are tested for both Reynolds numbers. In the table, N_i is the number of grid points in each direction and Δ_i^+ is the grid width in the wall unit. Because of the non-uniform distribution in y direction, the grid width at the channel center, Δy_c^+, is shown in Table 1.

The test filtering on the GS flow field is required in the dynamic procedure. Usually in the finite-difference method, the convolution integral of Eq.(5) is simplified for the computational convenience. Using the Taylor expansion for the Gaussian filter, $G(r;\Delta)=\sqrt{6/\pi\Delta^2}\exp(-6r^2/\Delta^2)$, the approximation

$$\tilde{\bar{f}}\left[\simeq \bar{f}+\frac{\bar{f}''}{2}\int_{-\infty}^{\infty} r^2 G(r;\tilde{\Delta})dr\right] \simeq \bar{f}+\frac{\tilde{\Delta}}{24}\bar{f}'', \qquad (16)$$

is derived (Leonard, 1974). The last term is obtained by the finite-difference method. In case of flow in a plane channel, the test filter is applied in the homogeneous (x and z) directions and not in the wall-normal direction because Δ_y is not uniform. Assuming the test-filter width in the homogeneous directions to be twice of the grid spacing, the ratio becomes $\alpha[=(\tilde{\Delta}_x\bar{\Delta}_y\tilde{\Delta}_z)^{1/3}/(\bar{\Delta}_x\bar{\Delta}_y\bar{\Delta}_z)^{1/3}]=4^{1/3}$.

Hereafter, 'OD model' denotes the one-equation dynamic model proposed in this study, 'S model' is the standard Smagorinsky model (1963) using $C_S=0.1$ with van Driest damping near the wall, 'O model' is the one-equation model (Okamoto and Shima, 1999). The common numerical method is used for LES with these models.

Results and Discussion

Figure 1 shows the relationship between the grid resolution, Δ_z^+, and the bulk velocity

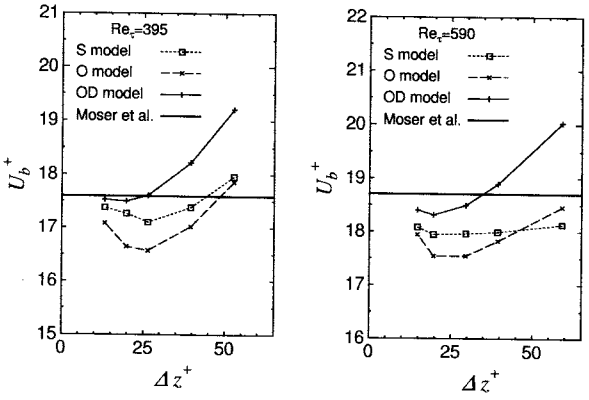

(a) $Re_\tau=395$ (b) $Re_\tau=590$

Figure 1: Influence of grid resolution: relationship between bulk velocity and grid resolution in spanwise directon

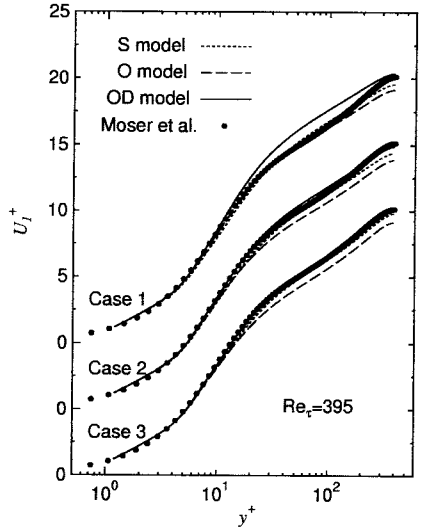

(a) $Re_\tau=395$

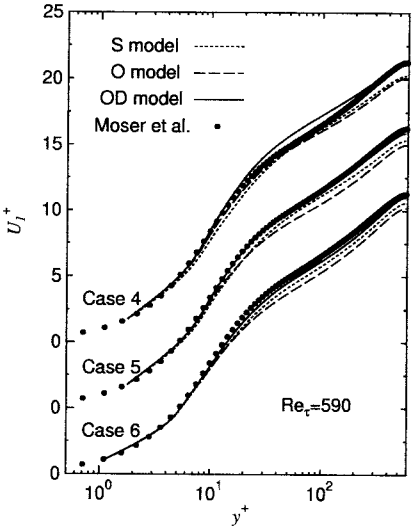

(b) $Re_\tau=590$

Figure 2: Mean streamwise velocity

$$U_b^+=\frac{1}{2\delta}\int_0^{2\delta}<u>dy. \qquad (17)$$

Figure 1 includes the results of higher and lower resolution cases than Cases 1~3 for $Re_\tau=395$ and Cases 4~6 for $Re_\tau=590$. As expected, results of all models converge on the DNS result by improving the grid resolution. In case of poor resolution, our OD model overestimates the flow rate. This is thought to be common feature of dynamic procedure implemented by the finite-difference method (Morinishi and Vasilyev, 2001). In case of finer grid, on the other hand, OD model shows best convergence to the DNS data. This tendency is evident especially for $\Delta z^+\leq 30$.

Figure 2 compares mean velocity profiles. The result of our OD model shows closest agreement with DNS database, except for Cases 1 and 4. Figure 3 shows intensity of velocity fluctuation. In Fig. 3(a), results of v_{rms} by S and OD models are almost same. The streamwise intensity, u_{rms}, is overestimated, while other components, v_{rms} and w_{rms}, are

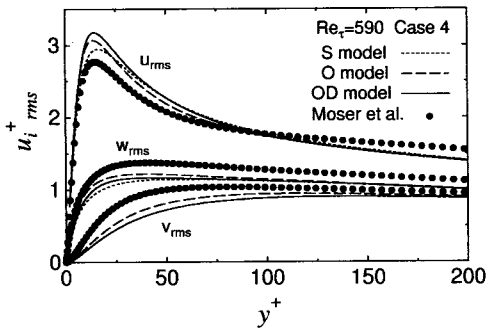

(a) Case 4

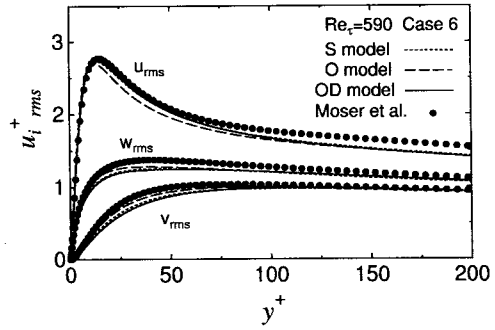

(b) Case 6

Figure 3: Intensity of velocity fluctuations at $Re_\tau = 590$

underestimated in case of poor resolution. This is a common feature in LES and DNS and is due to the lack of resolution for vortex structure in near-wall region. Results by finer grid are improved as shown in Fig. 3(b).

The asymptotical behavior of GS and SGS components of turbulence kinetic energy, K_{GS} and K_{SGS}, are shown in Fig. 4. K_{GS} should be proportional to $(y^+)^2$ in the vicinity of the plane wall. On the other hand, there is not such an requirement for K_{SGS} because it depend on the filter width $\bar{\Delta}$ that is commonly a function of distance from the wall. In any case, however, it is desirable K_{SGS} behaves in accordance with K_{GS}. For such a sense, the result shown in Fig. 4 seems reasonable.

Figure 5 shows the budget of SGS kinetic energy, namely average of each term in the transport equation of K_{SGS}. For the most part, the production is balanced with the dissipation. So the local equilibrium is satisfied for the ensemble average. In the vicinity of the wall, the production is replaced by the viscous diffusion. In our case, the addition of Eq. (15) played an important role to realize a reasonable profile of K_{SGS} and its budget in the near-wall region.

Finally we would like to mention about the increase in CPU time by introducing the dynamic procedure into a one-equation SGS model. But, please note that the additional part has not yet optimized for vector processors (NEC SX-4 and SX-5). About 70% was increased for simultaneous calculation for the transport equation of K_{SGS} (without dynamic procedure) and additional 70% was needed for the dynamic procedure of the energy production in K_{SGS}. The OD model therefore required CPU time about 2.5 times larger than that for the S model.

LES OF FLOW IN A ROTATING CHANNEL

A fully developed flow in a plane channel with constant

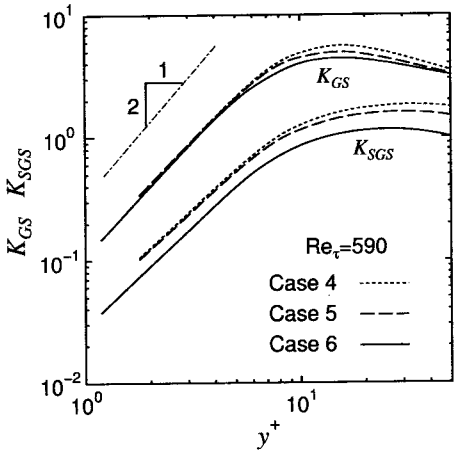

Figure 4: Near-wall behavior of GS and SGS turbulent kinetic energy at $Re_\tau = 590$

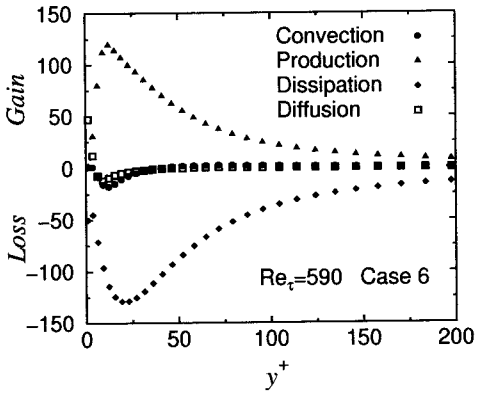

Figure 5: Budget of SGS kinetic energy at $Re_\tau = 590$ in Case 6

spanwise rotation, as shown in Fig. 6, has been extensively studied by LES (Miyake and Kajishima, 1986a and 1986b) and DNS (Kristoffersen and Andersson, 1993) because of the numerical convenience. Modulations in shear stress and turbulence intensity are caused by the Coriolis force. Furthermore, the secondary flow of the roll-cell type is observed in the mainstream. This is a typical example of turbulence phenomena affected by the body force, including an important feature of the flow in turbomachineries.

In the rotating channel, turbulence is enhanced in the pressure wall side and attenuated in the suction side. This is due to the shift of Reynolds stress profile caused by the Coriolis force. The result of LES using the Smagorinsky

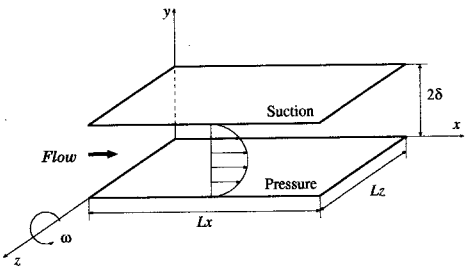

Figure 6: Rotating channel flow

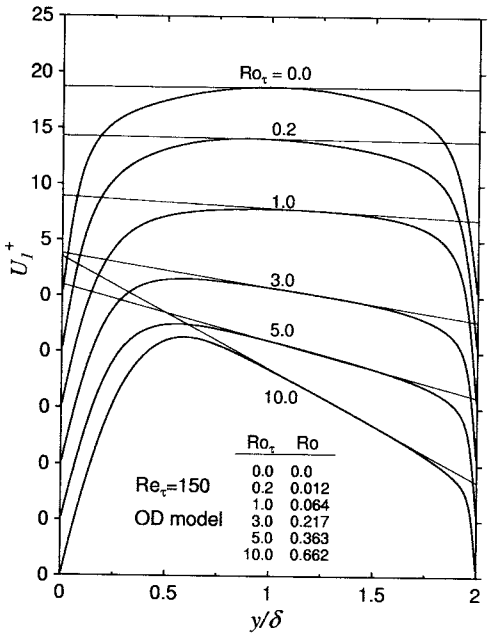

Figure 7: Mean streamwise velocity in the rotating channel by OD model

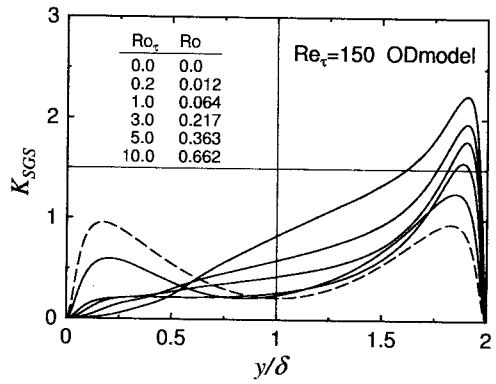

Figure 8: SGS turbulent energy in the rotating channel by OD model

model successfully reproduced this tendency (Miyake and Kajishima, 1986a and 1986b). At the same time, a defect of Smagorinsky model was exposed concerning to the re-laminarization in the suction side. In this side, turbulence disappears when the rotation is larger a certain rate. But the SGS eddy viscosity is given by the Smagorinsky model, $\nu_S = C_S\bar{\Delta}|\bar{S}_{ij}|$, because of the mean velocity gradient. The conventional one-equation model may not solve this because the mean velocity gradient gives SGS energy production. Thus some empirical modification is required for the primitive model.

The one-equation dynamic model proposed in our study is expected to remove this sort of inconsistency between the GS and SGS portions of turbulence energy. The main reason is that the production of SGS energy disappears automatically in the situation of re-laminarization of GS turbulence.

Outline of Computation

The filtered Navier-Stokes equation on a frame rotating

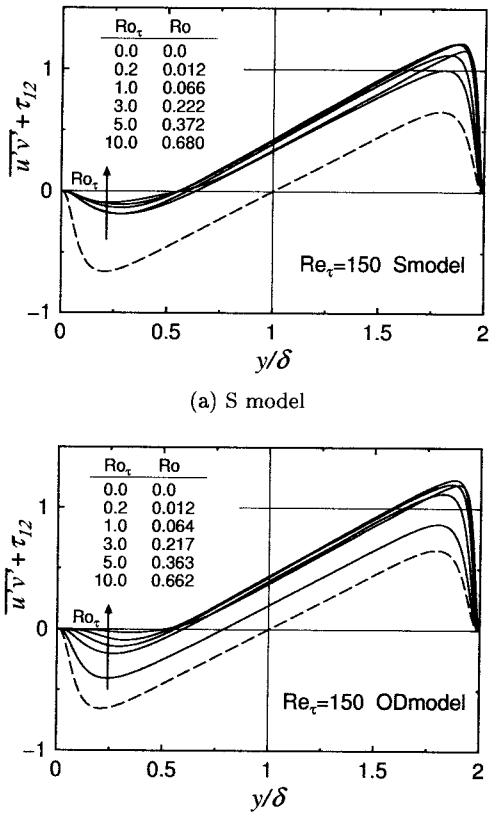

Figure 9: Reynolds shear stress profiles in the rotating channel (dashed lines represent the non-rotating cases)

at the constant angular velocity Ω is as follows,

$$\frac{\partial \bar{u}_i}{\partial t} + \bar{u}_j \frac{\partial \bar{u}_i}{\partial x_j} = 2\Omega(\delta_{i1}\bar{u}_2 - \delta_{i2}\bar{u}_1) - \frac{\partial}{\partial x_i}\left(\bar{P} - \frac{r^2\Omega^2}{2}\right) + \frac{\partial}{\partial x_j}(-\tau_{ij} + 2\nu\bar{S}_{ij}), \quad (18)$$

where δ is the Kronecker delta. The first term in the right hand side represents Coriolis force while the potential of centrifugal force is included in the pressure term.

The angular velocity Ω can be non-dimensionalized by the channel width 2δ and the wall friction velocity averaged on both sides, $u_\tau^2 = \frac{1}{2}\left(u_{\tau s}^2 + u_{\tau p}^2\right)$, as follows,

$$Ro_\tau = 2\Omega\delta/u_\tau \quad (19)$$

where $u_{\tau s}$ and $u_{\tau p}$ are wall friction velocities on the suction and pressure sides. The intensity of rotation is also represented by bulk velocity U_b

$$Ro = 2|\Omega|\delta/U_b = |Ro_\tau|u_\tau/U_b\,. \quad (20)$$

Our calculation was conducted for $Ro_\tau = 0 \sim 10$ at $Re_\tau = 150$. The computational domain is $L_x = 12.8\delta$, $L_y = 2\delta$, $L_z = 6.4\delta$ and the number of computational grid is $N_x = 48$, $N_y = 65$ and $N_z = 48$. The numerical method is same as that for non-rotating case.

Results and Discussion

Figure 7 shows the change of mean velocity profiles due to the rotation. When system rotation is imposed, the profile becomes asymmetric. Namely, the velocity gradient

decreases in the suction side ($x = 0$) and vice versa in the pressure side ($x = 2$). In the mainstream region, the neutral situation $S = -2\Omega/(dU_1/dy) = -1$ is observed which is corresponding to the former DNS (Kristoffersen and Andersson, 1993). The above relation derives $U_1^+ = 2\Omega y + C$. There seems the region of constant velocity gradient 2Ω and it becomes wider in accordance with the increase in Ro_τ. As shown in Fig. 7, the realization of this tendency is quite reasonable.

Figure 8 shows an influence of rotation on the SGS kinetic energy K_{SGS} obtained by our OD model. It increases in the pressure side and decreases in the suction side. As expected, K_{SGS} reaches zero in the suction side representing the re-laminarization tendency.

Figure 9 shows Reynolds shear stress (total of GS and SGS portion). The Reynolds stress reaches to zero in the suction side. In the result by S model, there remains Reynolds stress even for high rotation rate. As clearly shown, our OD model represents the SGS shear stress in the near-wall region of the rotating channel more correctly than S model.

CONCLUSIONS

The dynamic procedure is suitable for the determination of energy transfer between GS and SGS component. On the other hand, the SGS eddy-viscosity should depend on the subgrid scale kinetic energy. In this study, these matters have been incorporated by applying the dynamic procedure for the production term in the equation of SGS kinetic energy. Namely, the one-equation dynamic model is proposed. Furthermore, any empirical modification for SGS model was not required in our method. Especially, parameters such as the distance from the wall or wall friction velocity, which are hardly specified for complicated geometry, were not used.

The test by a fully developed flow in a plane channel proved the agreement between our model and established DNS database. When the grid spacing in the spanwise direction is less than 30 in wall unit, our OD model showed advantage over previous models. The OD model also showed the availability for the flow in a rotating channel.

The dynamic procedure sometimes gives negative production rate of SGS kinetic energy. It decrease K_{SGS} for some extent and indirectly affect the GS portion through the SGS eddy viscosity evaluated by K_{SGS}. In this process, any numerical instability was not caused. In our case, only the clipping for negative K_{SGS} was needed. But the fraction of clipped area was negligible and this treatment was unlikely to affect the numerical result. Although adopting the one-equation dynamic model increases the CPU time, it has a number of notable merits being in accordance with the scope of dynamic procedure.

REFERENCES

Davidson, L., 1997, "Large eddy simulation: A dynamic one-equation subgrid model for three-dimensional recirculating flow", *11th Int. Symp. on Turbulent Shear Flow*, Vol. 3, pp. 26.1-26.6.

Germano, M., Piomelli, U., Moin, P., and Cabot, W. H., 1991, "A dynamic subgrid-scale eddy viscosity model", *Phys. Fluids*, Vol. A3, No. 7, pp. 1760-64.

Ghosal, S., Lund, T. S., Moin, P. and Akselvoll, K., 1995, "A dynamic localization model for large-eddy simulation of turbulent flows", *J. Fluid Mech.*, Vol. 286, pp. 229-255.

Horiuti, K., 1985, "Large eddy simulation of turbulent channel flow by one-equation modeling", *J. Phys. Soc. Jpn.* Vol. 54, No. 8, pp. 2855-2866.

Horiuti, K., 1990, "Higher-order terms in the anisotropic representation of Reynolds stresses", *Phys. Fluids*, Vol. A2, No. 10, pp. 1708-1710.

Horiuti, K., 1993, "A proper velocity scale for modeling subgrid-scale eddy viscosities in large eddy simulation", *Phys. Fluids*, Vol. A5, No. 1, pp. 146-157.

Jones, W. P. and Launder, B. E., 1972, "The prediction of laminarization with a two-equation model of turbulence", *Int. J. Heat and Mass Transfer*, Vol. 15, pp. 301-314.

Kajishima, T. and Nomachi, T., 2003, "One-equation subgrid scale model using dynamic procedure for the energy production", to appear in *4th ASME-JSME Joint Fluids Engineering Conference, Honolulu*, (also submitted to *Trans. JSME*, Ser. B, in Japanese).

Kristoffersen, R. and Andersson, H., 1993, "Direct simulations of low-Reynolds-number turbulent flow in a rotationg channel", *J. Fluid Mech.*, Vol. 256, pp. 163-197

Leonard, A., 1974, "On the energy cascade in large-eddy simulation of turbulrnt fluid flows", *Adv. in Geophys.*, Vol. 18A, pp. 237-248.

Lilly, D. K., 1992, "A proposed modification of the Germano subgrid scale closure method", *Phys. Fluids*, Vol. A4, No. 3, pp. 633-635.

Miyake, Y. and Kajishima, T., 1986a, "Numerical Simulation of the Effects of Coriolis Force on the Structure of Turbulence: 1st Report, Global Effects", *Bull. JSME*, Vol. 29, No. 256, pp.3341-3346.

Miyake, Y. and Kajishima, T., 1986b, "Numerical Simulation of the Effects of Coriolis Force on the Structure of Turbulence: 2nd Report, Structure of Turbulence", *Bull. JSME*, Vol. 29, No. 256, pp.3347-3351.

Morinishi, Y. and Vasilyev, O. V., 2001, "A recommended modification to the dynamic two-parameter mixed subgrid scale model for large eddy simulation of wall bounded turbulent flow", *Phys. Fluids*, Vol. A13, No. 11, pp. 3400-3411.

Moser, R. D., Kim, J. and Mansour, N. N., 1999, "Direct numerical simulation of turbulent channel flow up to Re_τ=590", *Phys. Fluids*, Vol. A11, No. 4, pp. 943-945.

Okamoto, M. and Shima, N., 1999, "Investigation for the one-equation-type subgrid model with eddy-viscosity expression including the shear-dumping effect", *JSME Int. J.*, Vol. 42, No. 2, Ser.B, pp. 154-161.

Smagorinsky, J., 1963, "General circulation experiments with the primitive equations", *Mon. Weather Rev.*, Vol. 91, pp. 99-164.

Sohankar, A., Davidson, L. and Norberg, C., 2000, "Large eddy simulation of flow past a square cylinder: Comparison of different subgrid scale models", *Trans. ASME, J.Fluids Eng.*, Vol. 122, pp. 39-47.

Yoshizawa, A. and Horiuti, K., 1985, "A statistically-derived subgrid-scale kinetic energy model for the large-Eddy simulation of turbulent flows", *J. Phys. Soc. Jpn*, Vol. 54, No. 8, pp. 2834-2839.